Coupled electric and thermal batteries models using energetic macroscopic representation (EMR) for range estimation in electric vehicles

Ronan German, N. Solis, L. Reyes, L. Da Silva, F.-A. Lebel, Joao Trovao, A. Bouscayrol

HAL Id: hal-01948592

https://hal.science/hal-01948592

Submitted on 10 Dec 2018

Coupled Electric and Thermal Batteries Models using Energetic Macroscopic Representation (EMR) for Range Estimation in Electric Vehicles

R. German[1], N. Solis[1,2], L. Reyes[1,3], L. Silva[4], F.-A. LeBel[3], João P. Trovão[3], A. Bouscayrol[1],

[1] Univ. Lille, Centrale Lille, Arts et Métiers Paris Tech, HEI,
EA 2697 – L2EP - Laboratoire d'Electrotechnique et d'Electronique de Puissance, F-59000 Lille, France.
[2] Universidad Nacional de Río Cuarto, Córdoba – Argentina.
[3] e-TESC Lab, University of Sherbrooke, Sherbrooke, QC, J1K 2R1, Canada.
[4] Universidad Nacional de Rafaela, Argentina.
Corresponding author e-mail: Ronan.German@univ-lille1.fr
Tel.: +33 / (0) – 320.434157

Acknowledgements

Keywords

Abstract

Electric models of battery have to take into account the effect of temperature for the state-of-charge estimation. As a matter of fact, at low temperature the driving range of the vehicle can be overestimated up to more than 20% with electric only models. We propose to couple thermal and electric battery models for improving the range estimation.

1. Introduction

Electric Vehicles (EVs) are vehicles of the future. But they suffer of a lack of autonomy, a long charging time, and a high cost [1]. The range anxiety is key issue for EV's drivers [2]. Therefore, estimation of the correct driving range is an important matter.

In some cold winter countries, EV manufacturers noticed reduced driving range (autonomy) when temperature goes under 0 °C. For example, a Canadian study dealt with the influence of low temperature on battery with sub-zero temperatures. The result was a capacity decrease up to 35 % at -20 °C compared to 25 °C [3]. Other electric parameters (such as series resistance for instance…) also depend on the temperature [4]. These variations of battery behavior are non-permanent and the original driving range is reached when the temperature goes higher.

Moreover, cold and hot weathers both have an important effect on battery ageing rate. The result of ageing is a permanent decrease of the discharge capacitance (reduced driving range) and an increase of the battery resistance (increase of Joule losses). For subzero temperature, the ageing rate is drastically increased [5]. For temperatures from 10 °C to 60 °C it is commonly considered that the ageing rate doubles when the temperature increases by 10 °C [6]. Thus, estimating the temperature of the battery during one cycle is also very important for long term driving range.

The goal of this paper is to build an Electro-Thermal (ET) model of the battery with electric parameters thermal dependence to better estimate the driving range of the EVs under various

temperature conditions. This model is intended to be used for vehicle simulation and hardware in the loop for future works. Therefore, it must be as simple as possible to limit the calculation time.

Some papers have already proposed ET models focused on the battery impedance parameters evolution. For example, papers [4] and [7] include a temperature dependence on the series resistance of the battery. In this paper, the capacity thermal dependence (based on the experimental results of [3]) is also considered in order to better estimate the EV range.

First the classic electric and thermal models of Li-ion battery are presented. Then, they are associated using Energetic Macroscopic Representation (EMR) [8]. As EMR has already been used to model traction systems of EVs and HEVs (Hybrid Electric Vehicles) [9]-[10], such a formalism will enable an easy integration of this ET battery model for vehicle simulation. The experimental thermal dependence of the capacity and the series resistance of the battery is showed through literature results [3], [4]. The electric and thermal models are coupled using the EMR formalism. The electric parameters of the model are calculated with the thermal dependence extracted from the literature results. In a second time the model is validated by experimental results [4]. Finally, the range of an EV is tested at different temperatures.

2. Li-ion Batteries classical modeling

2.1. Classic Li-ion Electrical Model and EMR Organization

Different models can be found for batteries. The complexity of the models depends on the application. Some models are called electrochemical models. They are based on the kinetic of the energy storage reactions inside the battery. This type of model is the nearest from the chemistry of the system [11]. Therefore they can be used to monitor battery (ageing for example).

Equivalent circuit models are another kind of model. The battery electric behavior is represented by equivalent impedances and sources. Each electric parameter is linked with a phenomenon happening in the battery. For example, ionic transfer delays can be modeled by RC circuits [12] and ionic diffusion can be modelled by a constant phase element (CPE) [13].

From the EV point of view, the battery is considered as a power source subsystem. Therefore, the equivalent circuit model is adapted for EV application. For a matter of simplicity we neglect ionic transfer and diffusion. The cell dispersion (i.e. the slight differences for electric parameters between cells grouped in a battery [14]) is not considered as we just model a battery composed of one cell for this study. Therefore a simple Thevenin model is chosen. It consists in an open circuit voltage (OCV) dependent on the state-of-charge (SoC) and a series resistance R_{bat} (see Fig.2).
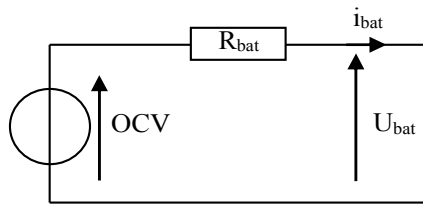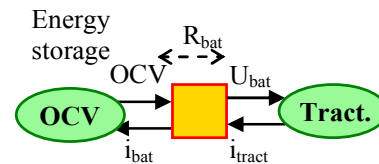

Fig. 1. Electric model for battery   Fig. 2. EMR organization of electric model

The SoC (in %) is frequently used as to quantify the energy stored in the batteries. It is calculated with the capacity of the battery C_{bat} (in Ah) which represents the current necessary to fully discharge the battery in one hour. It represents the remaining capacity stored in the battery over its maximum capacity C_{bat}.

$$SoC = SoC_{init} - \frac{\frac{1}{3600}\int_0^t i_{bat}\ dt}{C_{bat}} \times 100 \qquad (1)$$

Where SoC_{init} is the initial SOC (at t=0 s), i_{bat} is the discharge current and t is the time.

The EMR is a causal method to organize various models [8]. Four kinds of pictograms (see appendix) are used to describe basic energetic functions (energy source, accumulation, distribution and conversion). Each pictogram highlights the causal inputs and outputs of a component. The product of the input and output is the power transiting through the function described by the related pictograms.

The battery is considered as a voltage source and a conversion element. The voltage source (output OCV) takes as input the battery current i_{bat}. The power flowing out the voltage source is obtained by the product of OCV and i_{bat}. The resistance is described by an energy conversion element.

$$U_{bat} = OCV(SoC) - Ri_{bat} \qquad (2)$$

To simplify, the traction part of the vehicle is considered as a current source in this EMR (equivalent traction source).

Generally, the parameters of these electrical models are not considered temperature dependent even though the energy storage principle of the battery is dependent on the temperature. Thus, the accuracy of the electric model is reduced if the impact of temperature is neglected.

2.2. Li-ion Battery Thermal Modeling

For a matter of simplicity, strong hypotheses have been taken for thermal modeling [15] (see Fig. 3):

- The battery cell is considered cylindrical with a length far bigger than the diameter. It is placed in open air (at T_{amb} temperature).
- The battery is composed of two parts (core and surface) perfectly homogeneous with associated thermal capacitances C_{core} and C_{surf} (in J/K). The Biot number [16] quantifying the thermal gradient in the cell is neglected. Therefore, the temperature in the core is considered homogeneous. The thermal resistances (R_{cond} and R_{conv} (in K/W)) are located at the interfaces between two parts (core and surface for instance).
- The heat source is located at the center of the core. The series resistance R_{bat} is the only source of heat. Reversible heat sources linked to the entropic effect [13] will be neglected.
- The only heat transfer mechanisms considered are conduction for solids and convection for solid to gas. Radiations are neglected as the self-heating of batteries is moderate in EV.

These hypotheses will be validated in part 4.1 with experimental thermal results coming from ref. [4].The equivalent thermal circuit is given in Fig. 4. In equivalent thermal circuit power is equivalent to electric current and temperature is equivalent to voltage. The joule losses are a power generator (P_{heat}) and the ambient air is a source of temperature (T_{amb}).
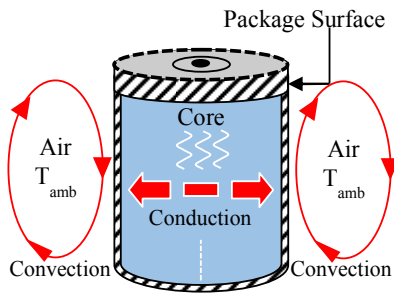

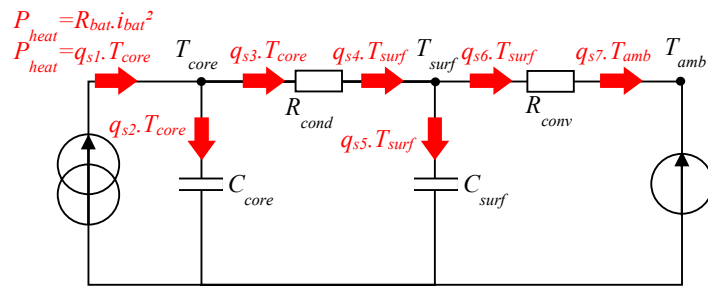Fig. 3. Heat transfer phenomena in the battery

Fig. 4. Equivalent thermal circuit

From a thermal point of view, the resistance R_{bat} is a component generating heat when a current goes through (Fig. 4). Thus, R_{bat} is described by a source of entropy flow q_{S1} in EMR (Fig. 5).

$$q_{S1} = \frac{R_{bat}.i_{bat}^2}{T_{core}} \qquad (3)$$

In the thermal domain, the flow variable is the entropy flow q_S (expressed in W/°K [17]) and the effort variable is the temperature (°K). Like in the electric domain, the product of the flow variable and the effort variable leads to the power. The battery thermal model can be considered as a source with the entropy flow as input and the inside battery temperature T_{core} as output. The EMR of the thermal model is given in Fig. 5. The thermal capacitances are energy accumulation elements and the thermal resistances are energy conversion elements. The air is considered as a temperature source (T_{amb}).
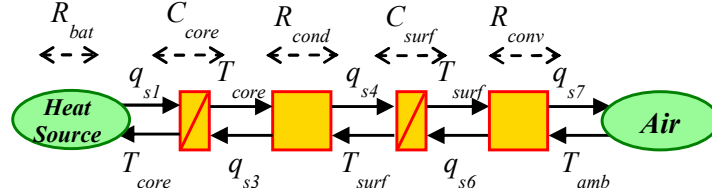

Fig. 5. EMR of the thermal model

The following equations are describing the behavior of the thermal model. As EMR is a causal representation, all the equations are expressed in a causal way (i.e. without derivative).

$$T_{core} = exp\left(\frac{1}{C_{core}} \int_0^t (q_{s1} - q_{s3})dt + ln(T_{core\ init})\right) \qquad (4)$$

$$qs3 = \frac{T_{core} - T_{surf}}{R_{cond} . T_{core}} \qquad (5)$$

$$qs4 = \frac{T_{core} - T_{surf}}{R_{cond} . T_{surf}} \qquad (6)$$

$$T_{surf} = exp\left(\frac{1}{C_{surf}} \int_0^t (q_{s4} - q_{s6})dt + ln(T_{surf\ init})\right) \qquad (7)$$

$$qs6 = \frac{T_{surf} - T_{amb}}{R_{conv} . T_{surf}} \qquad (8)$$

$$qs7 = \frac{T_{surf} - T_{amb}}{R_{conv} . T_{amb}} \qquad (9)$$

Where $T_{core\ init}$ and $T_{surf\ init}$ are the initial temperatures of the core and the surface of the battery. For the next parts, we consider that the battery is at rest for a long time at t=0s. Consequently, the initial core and surface temperatures are equal to T_{amb}.

3. Li-ion Batteries Electro-thermal modeling organized using EMR

3.1. Influence of Temperature on Li-ion Battery Electric Parameters

The experimental results presented in Fig. 6 and Fig. 7 are directly taken from [3] and [4]. They show that the electric parameters of the batteries are influenced by the temperature in the operating temperature range of the batteries:
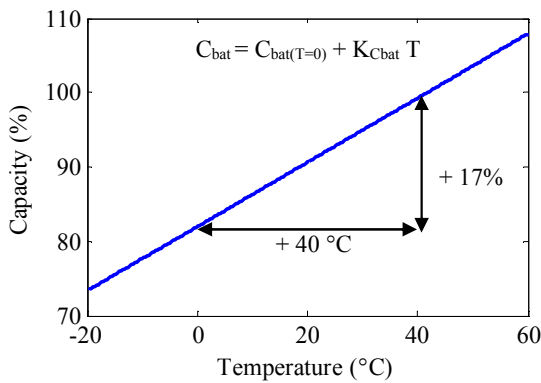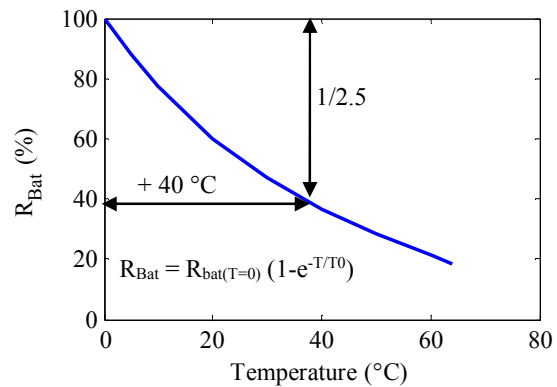

Fig. 6. Battery capacity evolution with temperature [3]

Fig. 7. Battery resistance evolution with temperature [4]

We notice that :

- C_{bat} increases linearly with temperature (impact on the EV range) [3].
- R_{bat} decreases exponentially with temperature (impact on the EV efficiency and range) [4].

3.2. EMR for Electro-Thermal (ET) Coupling

The common element between electric and thermal model is the resistance of the battery R_{bat} (see Fig. 8). The electric and thermal models are coupled by R_{bat} which is now a multi-domain (electro/thermal ET) coupling element. The temperature of the battery core T_{core} is used to update the value of C_{bat} and R_{bat}.
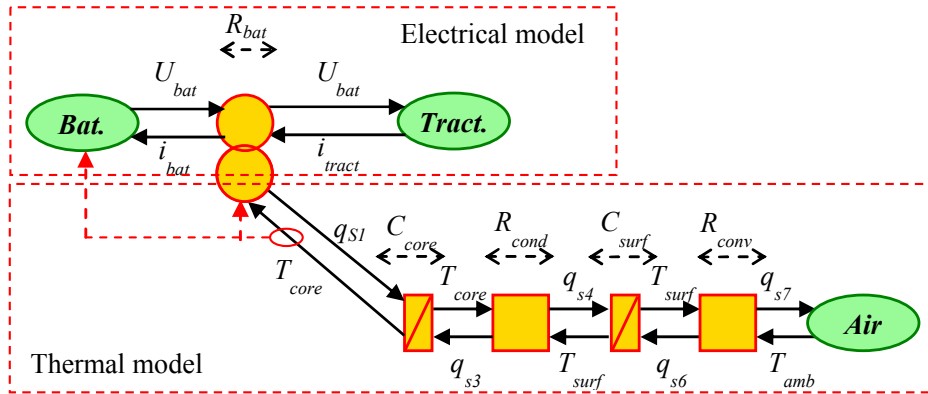

Fig. 8. EMR of the E/T model of the battery

4. Driving range estimation

4.1. Validation Using a Highly Dynamic Urban Assault Driving Cycle

The validation of the model is achieved with experimental results from the literature [4]. The tested cells are Lithium Iron Phosphate cells (Fig. 9) which is a technology used in EVs. The electric and thermal parameters are given in Table I. The thermal dependence is plotted in Fig. 6 and Fig. 7. The convection resistance is identified by [4] with a forced airflow (fan blowing) in a thermal chamber. The value extracted will vary as a function of the airflow.

Fig. 9. Studied Li-ion battery [18]

Parameters	Values
$U_{bat\ nom}$	3.3 V
C_{nom} @ 25°C	2.5 A.h
R_{nom} @ 25°C	16 mΩ
Max discharge rate	30 C
R_{cond}	2.18 (°K/W)
R_{conv}	3.33 (°K/W) (forced airflow)
C_{core}	67 (J/°K)
C_{surf}	4.5 (J/°K)

Table I: Parameters of the studied battery [4]

The model has been tested with the highly dynamic urban assault cycle (UAC) [4]. This cycle is expressed in C_{rate} in Fig 10 (1 C= 2.5 A). Then, the temperature given by the model has been compared with experimental results from [4]. The maximal error is lower than 2°C (i.e. 4 %) validating the accuracy of the E/T model (see Fig. 11).
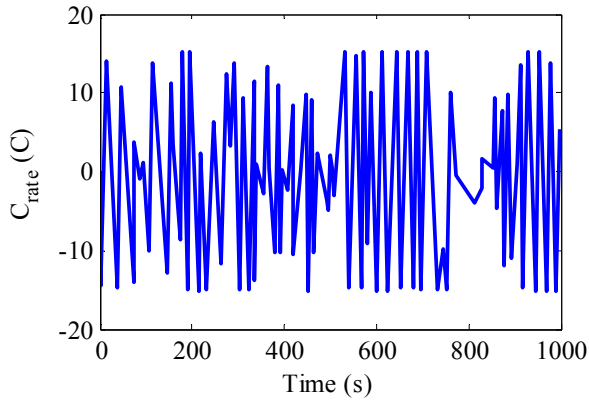
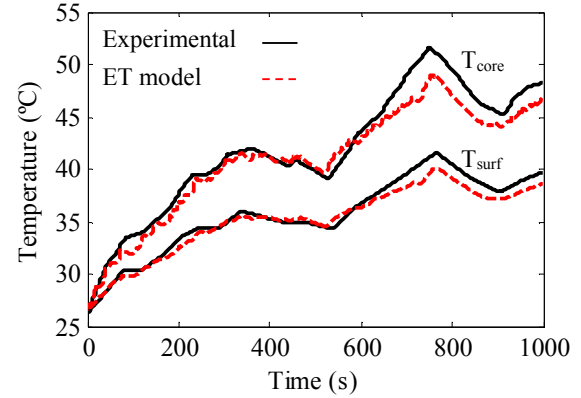Fig. 10. C rate of the urban assault cycle (UAC)

Fig. 11. Temperature evolutions for the UAC

4.2. Test of the Cells with the NEDC

The ET model is suited for any cycle with lower dynamics than the UAC. For a first EV range estimation, the New European Driving Cycle (NEDC) is considered. This cycle is composed of an urban part and an extra urban part (Fig. 12). The studied vehicle is the commercial Tazzari Zezo (2-seat vehicle of 600 kg) [19]. The parameters of the pure electric model of the battery are classically identified at 25 °C [18].

Fig. 13 presents the evolution of the estimated *SoC* during the NEDC for an ambient temperature of -20°C. Significant differences can be observed on the SOC estimation. For -20°C and one NEDC cycle the SOC variation of the ET model is + 22 % bigger than the SOC variation of the pure electric model.
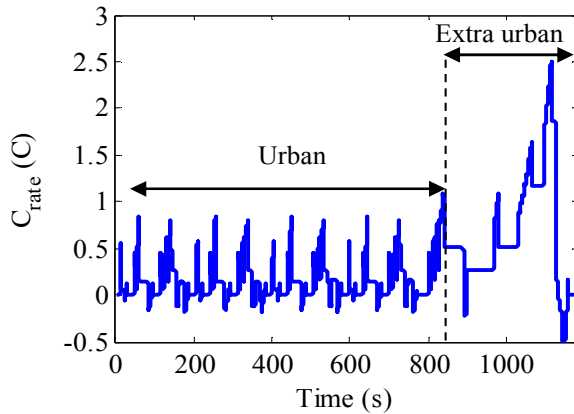

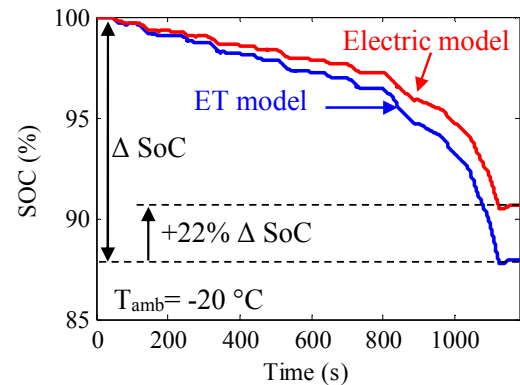Fig. 12. Crate during the NEDC

Fig. 13. SoC evolution of the NEDC

The process has been repeated for other temperatures (25°C and 40°C). Results are summarized in Table II.

Table II: Difference between electric and ET model for different ambient temperature after one NEDC (*SoC init* = 100%)

Ambient temperature	Electric model final *SoC*	ET model final *SoC*	Error on Δ *SoC*
-20 °C		88 %	+ 22 %
25 °C	90.6 %	90.65 %	- 0.5%
40 °C		91.3 %	- 8 %

With a pure electric battery model the *SoC* variation is underestimated by 22 %. The driving range will thus be overestimated by a significant factor. Thus, the ET model with capacity temperature

dependence is very useful for cold weather conditions. For 25°C the electric model gives satisfactory *SoC* estimation for NEDC cycle. Thus, at 25 °C temperature conditions the pure electric model is satisfactory for EV driving range estimation. For higher temperature (+40 °C) the driving range is under estimated by the electric model by a significant factor. Therefore, a part of the energy inside the battery is unused if the pure electric model is used for *SoC* estimation. Overall the ET model seems to be necessary for EV driving estimation as -20°C and + 40°C temperatures are encountered in many countries.
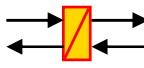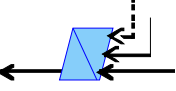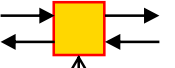
5. Conclusion

An electric model of a battery is coupled with a thermal model. This coupling enables an update of the electric parameters from the temperature evolution. This ET model has been validated by experimental results using a high-dynamics driving cycle. This model has then been used for a standard driving cycle for a small commercial EV.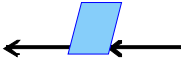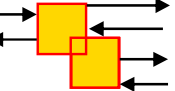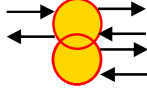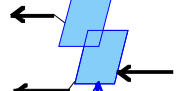 At low temperature, the driving range using a classical electric model is overestimated by about 20% and for high ambient temperature (40 °C) it is underestimated by about 10 %. The use of the ET model will thus improve the estimation of the driving range. This study is focused on one cell temperature. As perspective, the temperature interaction between cells in a battery pack can be considered [20].

References

[1] C. C. Chan, "Overview of electric, hybrid and fuel vell vehicles", Chapter 51, Encyclopedia of Automotive Engineering, John Willys & Sons, Ltd, 2015.

[2] J. Neubauer, E. Wood, "The impact of range anxiety and home, workplace and public charging infrastructure on simulated battery EV lifetime utility", *Journal of Power Sources*, no. 257, pp. 12-20, Jan. 2014.

[3] J. Jaguemont, L. Boulon, Y. Dube and D. Poudrier, "Low Temperature Discharge Cycle Tests for a Lithium Ion Cell," *2014 IEEE Vehicle Power and Propulsion Conference (VPPC)*, Coimbra,, pp. 1-6, 2014.

[4] X. Lin *et al.*, "Online Parameterization of Lumped Thermal Dynamics in Cylindrical Lithium Ion Batteries for Core Temperature Estimation and Health Monitoring," in *IEEE Transactions on Control Systems Technology*, vol. 21, no. 5, pp. 1745-1755, Sept. 2013.

[5] J. Jaguemont, L. Boulon, P. Venet, Y. Dube, and A. Sari, "Lithium-Ion Battery Aging Experiments at Subzero Temperatures and Model Development for Capacity Fade Estimation," *IEEE Trans. Veh. Technol.*, vol. 65, no. 6, pp. 4328–4343, Jun. 2016.

[6] I. Baghdadi, O. Briat, J.-Y. Delétage, P. Gyan, and J.-M. Vinassa, "Lithium battery aging model based on Dakin's degradation approach," *J. Power Sources*, vol. 325, pp. 273–285, Sep. 2016.

[7] Xinfan Lin, Hector E. Perez, Shankar Mohan, Jason B. Siegel, Anna G. Stefanopoulou, Yi Ding, Matthew P. Castanier, A lumped-parameter electro-thermal model for cylindrical batteries, Journal of Power Sources, Volume 257, Pages 1-11, July 2014.

[8] A. Bouscayrol, J. P. Hautier, and B. Lemaire-Semail, "Graphic Formalisms for the Control of Multi-Physical Energetic Systems: COG and EMR", Systemic Design Methodologies for Electrical Energy Systems, Chap. 3, Wiley-ISTE, ISBN 9781848213883, Oct. 2012.

[9] A. Castaings, W. Lhomme, R. Trigui, A. Bouscayrol,, "Real-time energy management strategies of a battery/supercapacitors system for Electric Vehicle under limitations", *Applied Energy*, Vol. 163, pp.190–200, February 2016..

[10] K. Chen, A. Bouscayrol, W. Lhomme, "Energetic Macroscopic Representation and Inversion-based control: Application to an Electric Vehicle with an electrical differential", *Journal of Asian Electric Vehicles*, vol. 6, no.1, pp. 1097-1102, June 2008.

[11] R. Ahmed, M. El Sayed, I. Arasaratnam, J. Tjong, and S. Habibi, "Reduced-Order Electrochemical Model Parameters Identification and State of Charge Estimation for Healthy and Aged Li-Ion Batteries—Part II: Aged Battery Model and State of Charge Estimation," *IEEE J. Emerg. Sel. Top. Power Electron.*, vol. 2, no. 3, pp. 678–690, Sep. 2014.

[12] I. Baghdadi, O. Briat, A. Eddahech, J. M. Vinassa, I. Baghdadi, and P. Gyan, "Electro-thermal model of lithium-ion batteries for electrified vehicles applications," presented at the The IEEE International Symposium on Industrial Electronics, pp. 1248–1252, 2015.

[13] A. Eddahech, O. Briat, and J.-M. Vinassa, "Thermal characterization of a high-power lithium-ion battery: Potentiometric and calorimetric measurement of entropy changes," *Energy*, vol. 61, pp. 432–439, Nov. 2013.

[14] F.-A. LeBel, S. Wilke, B. Schweitzer, M.-A. Roux, S. Al-Hallaj, and J. P. F. Trovao, "A Lithium-Ion Battery Electro-Thermal Model of Parallellized Cells," presented at the Vehicular Technology Conference (VTC-Fall), 2016 IEEE 84th, pp. 1–6, 2016.

[15] C. Forgez, D. Vinh Do, G. Friedrich, M. Morcrette, and C. Delacourt, "Thermal modeling of a cylindrical LiFePO4/graphite lithium-ion battery," *J. Power Sources*, vol. 195, no. 9, pp. 2961–2968, mai 2010.

[16] R. Mahamud and C. Park, "Spatial-resolution, lumped-capacitance thermal model for cylindrical Li-ion batteries under high Biot number conditions," *Appl. Math. Model.*, vol. 37, no. 5, pp. 2787–2801, Mar. 2013.

[17] L. Horrein, A. Bouscayrol, W. Lhomme, and C. Depature, "Impact of heating system on the range of an electric vehicle," *IEEE Trans. Veh. Technol.*, 2016

[18] A123 Systems, "Nanophosphate® High Power Lithium Ion Cell ANR26650M1-B.", 2011.

[19] Tazzari Zero website: http://www.tazzari-zero.com/index.html, website visited on March 2016.

[20] A. Hijazi, E. Bideaux, P. Venet and G. Clerc, "Electro-thermal sizing of supercapacitor stack for an electrical bus: Bond graph approach," *2015 Tenth International Conference on Ecological Vehicles and Renewable Energies (EVER)*, Monte Carlo, pp. 1-8, 2015.

APPENDIX: EMR PICTOGRAMS

(name)	source element (energy source)		accumulation element (energy storage)		Indirect inversion (closed-loop control)
	Mono-domain conversion element		Multi-domain conversion element		Direct inversion (open-loop control)
	Mono-domain coupling element (energy distribution)		Multi-domain coupling element (energy distribution)		coupling inversion (energy criteria)